istry: Carbohydrates, S. M. Hecht, Ed. (Oxford Univ. Press, New York, 1999), pp. 134–173.
3. P. Vogel, in *Glycoscience*, B. O. Fraser-Reid, K. Tatsuta, J. Thiem, Eds. (Springer, Berlin, 2001), vol. 2, pp. 1023–1174.
4. S. Y. Ko, A. W. M. Lee, S. Masamune, L. A. Reed, K. B. Sharpless, *Science* **220**, 949 (1983).
5. S. J. Danishefsky, C. J. Maring, *J. Am. Chem. Soc.* **107**, 7761 (1985).
6. D. L. Boger, K. D. Robarge, *J. Org. Chem.* **53**, 5793 (1988).
7. L. F. Tietze, A. Montenbruck, C. Schneider, *Synlett.* **1994**, 509 (1994).
8. M. Takeuchi, T. Taniguchi, K. Ogasawara, *Synthesis* **1999**, 341 (1999).
9. C. Bataille *et al.*, *J. Org. Chem.* **67**, 8054 (2002).
10. S. G. Davies, R. L. Nicholson, A. D. Smith, *Synlett.* **2002**, 1637 (2002).
11. A. B. Northrup, D. W. C. MacMillan, *J. Am. Chem. Soc.* **124**, 6798 (2002).
12. M. Movassaghi, E. N. Jacobsen, *Science* **298**, 1904 (2002).
13. B. List, *Tetrahedron* **58**, 5573 (2002).
14. B. List, R. A. Lerner, C. F. Barbas, III, *J. Am. Chem. Soc.* **122**, 2395 (2000).
15. Z. G. Hajos, D. R. Parrish, *J. Org. Chem.* **39**, 1615 (1974).
16. U. Eder, G. Sauer, R. Wiechert, *Angew. Chem. Int. Ed. Engl.* **10**, 496 (1971).
17. A. B. Northrup, I. K. Mangion, F. Hettche, D. W. C. MacMillan, *Angew. Chem. Int. Ed. Engl.* **43**, 2152 (2004).
18. For an example of Lewis base–catalyzed aldol reactions using trichlorosilylenolethers, see (*20*).
19. It should be noted that both the labeled enolsilane and TIPS dimer precursor were available in gram quantities from only 1.00 g of ethylene glycol ($31/mmol).
20. S. E. Denmark, S. K. Ghosh, *Angew. Chem. Int. Ed.*, **40**, 4759 (2001).
21. Financial support was provided by the NIH National Institute of General Medical Sciences (R01 GM66142-01) and gifts from Bristol-Myers Squibb, Johnson and Johnson, Eli Lilly, and Merck Research Laboratories. D.W.C.M. is grateful for support from the Camille and Henry Dreyfuss Foundation, the Sloan Foundation, and Research Corporation under the Cottrell Scholarship and Research Innovation programs. A.B.N. is grateful for an NSF predoctoral fellowship.

Supporting Online Material
www.sciencemag.org/cgi/content/full/1101710/DC1
Materials and Methods

21 June 2004; accepted 22 July 2004
Published online 12 August 2004;
10.1126/science.1101710
Include this information when citing this paper.

A Stable Compound Containing a Silicon-Silicon Triple Bond

Akira Sekiguchi,* Rei Kinjo, Masaaki Ichinohe

The reaction of 2,2,3,3-tetrabromo-1,1,4,4-tetrakis[bis(trimethylsilyl)methyl]-1,4-diisopropyltetrasilane with four equivalents of potassium graphite (KC_8) in tetrahydrofuran produces 1,1,4,4-tetrakis[bis(trimethylsilyl)methyl]-1,4-diisopropyl-2-tetrasilyne, a stable compound with a silicon-silicon triple bond, which can be isolated as emerald green crystals stable up to 100°C in the absence of air. The Si≡Si triple-bond length (and its estimated standard deviation) is 2.0622(9) angstroms, which shows half the magnitude of the bond shortening of alkynes compared with that of alkenes. Unlike alkynes, the substituents at the Si≡Si group are not arranged in a linear fashion, but are trans-bent with a bond angle of 137.44(4)°.

Hydrocarbons containing C=C double bonds (alkenes) and C≡C triple bonds (alkynes) form an abundant and structurally diverse class of organic compounds. However, the ability of heavier congeners of carbon (where element E is Si, Ge, Sn, and Pb) to form double bond of the type >E=E< and triple bond of the type -E≡E- was for a long time doubted (*1–4*). The first attempts to generate such species were unsuccessful, resulting in the formation of polymeric substances. This led to the often-cited "double-bond rule": Those elements with a principal quantum number equal to or greater than three are not capable of forming multiple bonds because of the considerable Pauli repulsion between the electrons of the inner shells (*5–7*). Such a viewpoint prevailed despite the accumulation of a vast amount of experimental data supporting the existence of multiply bonded species as reactive intermediates (*1–4*). This conflict was resolved nearly 30 years ago, when Lappert and Davidson reported the synthesis of the stable distannene $[(Me_3Si)_2CH]_2Sn{=}Sn[CH(SiMe_3)_2]_2$, where Me is methyl, which has a Sn=Sn double bond in the solid state (*8*). The next important discoveries came from two research groups in 1981: West and colleagues reported the synthesis of a stable compound with a Si=Si double bond, tetramesityldisilene (*9*), and Brook *et al.* synthesized a compound with a Si=C double bond (*10*). As for triple bonds, Power and co-workers recently prepared alkyne analogs of the heavier group 14 elements: germanium, tin, and lead (*11–13*). However, despite bearing nominal triple bonds, these compounds actually exhibited a highly pronounced nonbonding electron density character at the central atoms, resulting in a decrease in the bond order on descending group 14 (*14*, *15*). In light of these results, isolation of the silicon analog of alkynes has been a compelling goal. Although the theoretical analysis predicted the experimental accessibility of disilynes with a silicon-silicon triple

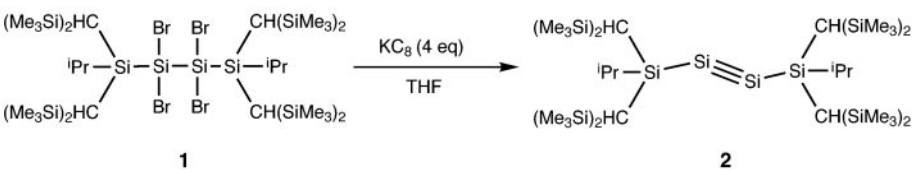

Reaction 1.

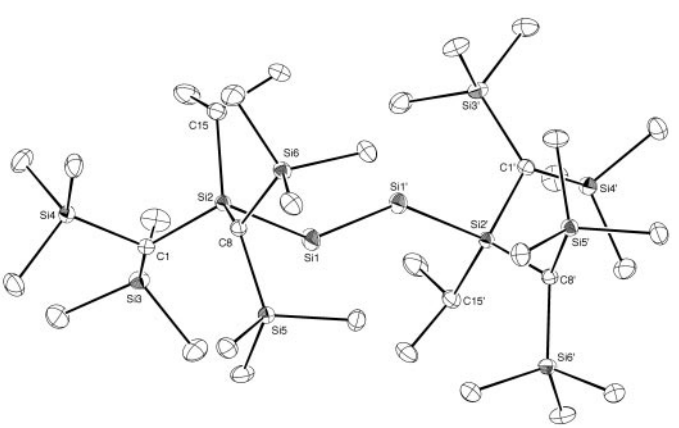

Fig. 1. Molecular structure of 1,1,4,4-tetrakis[bis(trimethylsilyl)methyl]-1, 4-diisopropyl-2-tetrasilyne (**2**) (30% probability ellipsoids for Si and C). Selected bond lengths (Å): Si1–Si1′ = 2.0622(9), Si1–Si2 = 2.3698(6), Si2–C1 = 1.9119(15), Si2–C8 = 1.9120(15), and Si2–C15 = 1.9180(16). Selected bond angles (°): Si1′–Si1–Si2 = 137.44(4), Si1–Si2–C1 = 108.97(5), Si1–Si2–C8 = 108.38(5), Si1–Si2–C15 = 106.47(5), C1–Si2–C8 = 106.83(6), C8–Si2–C15 = 114.77(7), and C1–Si2–C15 = 111.30(7). Estimated standard deviations are in parentheses.

Department of Chemistry, Graduate School of Pure and Applied Sciences, University of Tsukuba, Tsukuba, Ibaraki 305–8571, Japan.

*To whom correspondence should be addressed. E-mail: sekiguch@staff.chem.tsukuba.ac.jp

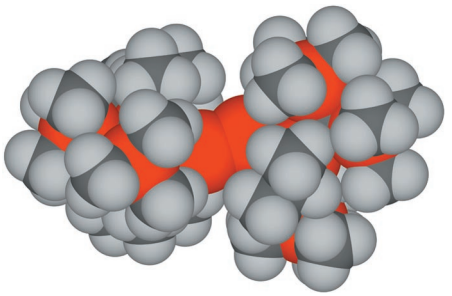

Fig. 2. Space-filling model of **2**. Si, red; C, gray; H, white.

bond (*16*), all attempts to isolate such postulated molecules have been unsuccessful (*17–19*). The difficulty in synthesizing disilynes is due in large part to their high reactivities, especially toward isomerization and dimerization.

We report the isolation and full characterization of 1,1,4,4-tetrakis[bis(trimethylsilyl)methyl]-1,4-diisopropyl-2-tetrasilyne **2**, a stable disilyne R-Si≡Si-R, which is the Si analog of an alkyne. In this compound, the Si≡Si triple bond is kinetically and thermodynamically stabilized by two large silyl substituents, each bearing one isopropyl and two bis(trimethylsilyl)methyl groups. The compound is accessed by reduction of a tetrabrominated precursor. Thus, the reaction of 2,2,3,3-tetrabromo-1,1,4,4-tetrakis[bis(trimethylsilyl)methyl]-1,4-diisopropyltetrasilane **1** with four equivalents of potassium graphite (KC_8) in dry tetrahydrofuran (THF) produces a dark green mixture, from which disilyne **2** can be isolated as extremely air- and moisture-sensitive emerald green crystals in 73% isolated yield (Reaction 1) (*20*, *21*). Despite the large steric congestion, the debromination reaction proceeds rapidly and cleanly. The disilyne **2** was purified by recrystallization from pentane at –30°C; it has a decomposition point of 127° to 128°C. No evidence for the isomerization of **2** to RRSi=Si or dissociation into the two RSi fragments (where R is $Si^iPr[(CH(SiMe_3)]_2$ and ^iPr is isopropyl) was observed, indicating that the two central Si atoms are strongly bonded.

The disilyne **2** was fully characterized spectroscopically; the most informative data came from ^{29}Si nuclear magnetic resonance (NMR) studies. Four equal-intensity resonance signals at the chemical shifts δ = –0.3, 0.0, 20.7, and 89.9 parts per million (ppm) were observed in the ^{29}Si NMR spectrum, assigned as follows: The peak at 89.9 ppm corresponds to a triply bonded Si atom, the peak at 20.7 ppm corresponds to Si atoms bonded to the Si≡Si group, and peaks at –0.3 and 0.0 ppm correspond to the four $CH(SiMe_3)_2$ groups (*21*). The resonance of the sp-hybridized Si atoms is shifted upfield compared with that of silyl-substituted disilenes (δ = 142.1 to 154.5 ppm) (*22*), as was observed in the case of ^{13}C NMR chemical shifts of silyl-substituted alkenes (δ = 188 to 197 ppm) and alkynes (δ = 112 to 114 ppm) (*23*).

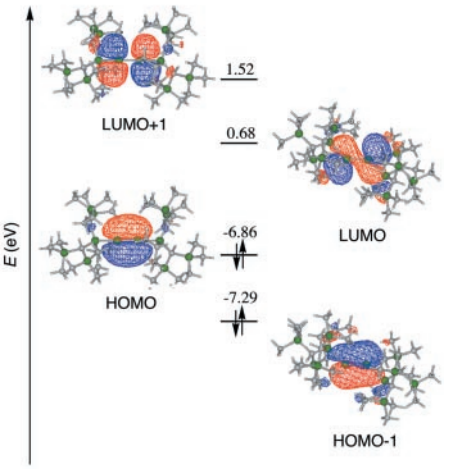

Fig. 3. The π MOs of **2** calculated at the HF/6-311G(d)//B3LYP/6-31G(d) level (HOMO-1, HOMO, LUMO, and LUMO+1). E is the energy level of the orbitals. The large vertical arrow indicates the energy level. The two small arrows indicate two electrons of opposing spin, referred to as paired electrons.

The solid state structure of **2** was confirmed by x-ray crystallographic analysis (Fig. 1). Full metrical parameters are listed in table S3 (*24*). The four Si atoms (Si2, Si1, Si1′, and Si2′) are perfectly coplanar and the bulky $Si^iPr[(CH(SiMe_3)]_2$ groups protect the central Si≡Si triple bond. The most significant result is the Si≡Si triple-bond length of 2.0622(9) Å. This value is 3.8% shorter than typical Si=Si double-bond length (2.14 Å) and 13.5% shorter than the average Si-Si single-bond length of 2.34 Å (*4*). This shortening is half the magnitude of that in the carbon counterparts. Moreover, alkynes have a linear geometry around the C≡C triple bond, whereas disilynes have been predicted to have a highly pronounced trans-bent geometry around the Si≡Si triple bond (*14*, *16*). The structure confirms this prediction: The substituents at the Si≡Si are not arranged in a linear fashion, but are trans-bent with a bond angle of 137.44(4)°, as determined by the Si2-Si1-Si1′ angle. This bond angle is 12.5° smaller than that calculated for HSi≡SiH (124.9°). According to theoretical investigations, substitution by electropositive silyl groups leads to a less trans-bent disilyne structure (*25*). The structure of **2** presented here is close to that predicted by a recent density functional (DFT) calculation on $(^tBu_3Si)_2MeSiSi{\equiv}SiSiMe(Si^tBu_3)_2$, where ^tBu is *tert*-butyl (*26*).

The space-filling model of **2** shown in Fig. 2 highlights the steric protection of the Si≡Si group by the isopropyl and bis(trimethylsilyl)methyl substituents. Upon replacement of the isopropyl groups in precursor with methyls, the reaction to produce the disilyne yields a dimerization product instead, bearing a tetrasilatetrahedrane core (*27*).

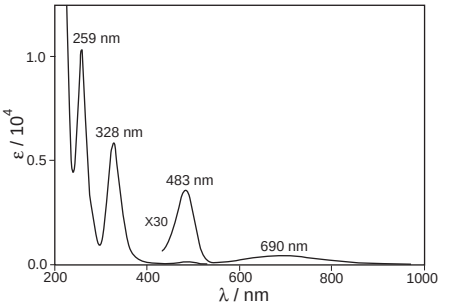

Fig. 4. Ultraviolet-visible absorption spectrum of **2** in hexane at room temperature; ε is the molar extinction coefficient ($dm^3\ mol^{-1}\ cm^{-1}$).

Despite the steric protection, the Si≡Si triple bond in **2** does undergo addition reactions with a halogen. Thus, **2** readily reacted with two equivalents of bromine at room temperature in hexane to form **1** in 94% yield by cleavage of the two π(Si≡Si) bonds.

A DFT calculation on disilyne **2** at the B3LYP/6-31G(d) level of theory well reproduces the experimental geometry and the structural parameters (calculated value: 2.093 Å for the Si≡Si bond length, 136.1° for the trans-bending angle). The molecular orbitals (MOs) of **2** calculated at the HF/6-311G(d)//B3LYP/6-31G(d) level presented in Fig. 3 show two nondegenerate highest occupied π MOs (HOMO-1 and HOMO) and two lowest unoccupied antibonding π* MOs (LUMO and LUMO+1). The out-of-plane HOMO and LUMO+1 are represented by the pure (p_z-p_z) π MOs, whereas the in-plane HOMO-1 and LUMO are represented mainly by (p_y-p_y) π MOs with a slight contribution from the antibonding σ* (Si-Si) orbital of the central bond. In accordance with the triple-bond structure, natural bond orbital analysis of **2** shows electron occupation of the two π(Si≡Si) orbitals (1.934 and 1.897 electron), indicating their bonding character. The bond order (Wiberg bond index) of Si1-Si1′ is 2.618, which agrees with the real Si≡Si triple bond. The presence of the two nondegenerate π and two π* MOs in **2** is reflected in the ultraviolet-visible absorption of **2**, as shown in Fig. 4. The strong absorption bands at wavelengths (λ) of 259 and 328 nm are due to the two allowed π-π* transitions. The weak absorption bands with maxima of 483 and 690 nm are probably a result of forbidden transitions, and the latter very weak one (HOMO-LUMO transition) is responsible for the emerald green color of **2**.

References and Notes

1. R. West, *Angew. Chem. Int. Ed. Engl.* **26**, 1201 (1987).
2. G. Raabe, J. Michl, in *The Chemistry of Organic Silicon Compounds*, S. Patai, Z. Rappoport, Eds. (Wiley, New York, 1989), part 2, chap. 17.

3. P. P. Power, *Chem. Rev.* **99**, 3463 (1999).
4. M. Weidenbruch, *The Chemistry of Organic Silicon Compounds*, Z. Rappoport, Y. Apeloig, Eds. (Wiley, Chichester, UK, 2001), vol. 3, chap. 5.
5. E. Wiberg, *Lehrbuch der Anorganischen Chemie*, A. F. Holleman, E. Wiberg, Eds. (W. de Gruyter, Berlin, Germany, eds. 22 and 23, 1943).
6. J. Goubeau, *Angew. Chem.* **69**, 77 (1957).
7. P. Jutzi, *Angew. Chem. Int. Ed. Engl.* **14**, 232 (1975).
8. P. J. Davidson, M. F. Lappert, *J. Chem. Soc. Chem. Commun.* **1973**, 317 (1973).
9. R. West, M. J. Fink, J. Michl, *Science* **214**, 1343 (1981).
10. A. G. Brook, F. Abdesaken, B. Gutekunst, G. Gutekunst, R. K. Kallury, *J. Chem. Soc. Chem. Commun.* **1981**, 191 (1981).
11. (2,6-Tip_2-C_6H_3)PbPb(C_6H_3-2,6-Tip_2), where Tip is 2,4,6-*i*-Pr_3-C_6H_2-, is described in L. Pu, B. Twamley, P. P. Power, *J. Am. Chem. Soc.* **122**, 3524 (2000).
12. (2,6-$Dipp_2$-C_6H_3)SnSn(C_6H_3-2,6-$Dipp_2$), where Dipp is 2,6-*i*-Pr_2-C_6H_3-, is described in A. D. Philips, R. J. Wright, M. M. Olmstead, P. P. Power, *J. Am. Chem. Soc.* **124**, 5930 (2002).
13. (2,6-$Dipp_2$-C_6H_3)GeGe(C_6H_3-2,6-$Dipp_2$)$_2$ is described in M. Stender, A. D. Phillips, R. J. Wright, P. P. Power, *Angew. Chem. Int. Ed. Engl.* **41**, 1785 (2002).
14. P. P. Power, *Chem. Commun.* **2003**, 2091 (2003).
15. G. H. Robinson, *Acc. Chem. Res.* **32**, 773 (1999).
16. S. Nagase, K. Kobayashi, N. Takagi, *J. Organomet. Chem.* **611**, 264 (2000).
17. A. Sekiguchi, S. S. Zigler, R. West, *J. Am. Chem. Soc.* **108**, 4241 (1986).
18. R. Pietschnig, R. West, D. R. Powell, *Organometallics* **19**, 2724 (2000).
19. The reduction of ($^tBu_3Si$)$_2$MeSiClSi=SiClSiMe(Si^tBu_3)$_2$ with lithium naphthalene in THF has recently been reported (*28*). This contains an unstable product with a low field ^{29}Si NMR signal at δ = 91.5 ppm, which was ascribed to a Si≡Si triple-bond resonance.
20. Crystals of **1** (100 mg, 0.087 mmol) and KC_8 (50 mg, 0.370 mmol) were placed in a glass tube and degassed. Dry oxygen-free THF (2 ml) was introduced by vacuum transfer and the mixture was allowed to warm from –78°C to room temperature overnight with stirring. The solution turned an intense green color. The solvent was replaced by hexane, and then the resulting potassium salt and graphite were filtered off in a glove box (a box equipped with gloves in which air- and moisture-sensitive compounds can be handled). After evaporation of the solvent, pentane was added and the solution was cooled at –30°C to give emerald green crystals of **2** (53 mg, 73%).
21. NMR of **2** ([D_6]benzene solution, ^{1}H) δ values (ppm): –0.01 (singlet, 4H), CH protons; 0.39 (singlet, 36H), $SiMe_3$ protons; 0.57 (singlet, 36H), $SiMe_3$ protons, 1.44 (doublet, 12H, spin-spin coupling constant J = 6.0 Hz, 12H), isopropyl methyl protons, 1.49 (septet, spin-spin coupling constant J = 6.0 Hz, 2H), isopropyl methyne proton. NMR (^{13}C) δ values: 5.1, 5.7, 8.9, 17.8, and 22.3. NMR (^{29}Si) δ values: –0.3, 0.0, 20.7, and 89.9. High-resolution mass spectrum: mass-to-charge ratio (m/z) calculated for $C_{34}H_{90}Si_{12}$ to be 834.4274, experimentally found to be 834.4275. Ultraviolet-visible spectrum (in hexane solution): λ_{max} [wavelength, molar extinction coefficient (ε)/dm^3 mol^{-1} cm^{-1}] 259, 10300; 328, 5800; 483, 120; and 690, 14.
22. M. Kira, T. Maruyama, C. Kabuto, K. Ebata, H. Sakurai, *Angew. Chem. Int. Ed. Engl.* **33**, 1489 (1994).
23. H. Sakurai, H. Tobita, Y. Nakadaira, *Chem. Lett.* **1982**, 1251 (1982).
24. An emerald green crystal (approximate dimensions, 0.30 by 0.15 by 0.15 mm) of **2** was used for the x-ray diffraction data collection on a Mac Science DIP2030K Image Plate Diffractometer with graphite-monochromatized Mo–K_α radiation (λ = 0.71070 Å). Cell constants and an orientation matrix for data collection corresponded to the monoclinic space group *C*2/*c*, with a = 30.9620(11) Å, b = 10.9060(2) Å, c = 18.1170(7) Å, β = 118.995(2)°, V = 5350.8(3) Å^3, four molecules per unit cell, formular weight 836.14, and calculated density 1.038 Mg/m^3. Data were collected at 120 K, θ range from 2.18° to 28.01°. There were 26,993 collected reflections (6412 unique, R_{int} = 0.0290); R_1 = 0.0373 for 5479 reflections with I > 2σ(I), wR_2 = 0.1096 for all reflections. More crystallographic data are available at the Cambridge Crystallographic database, accession code and deposition no. CCDC 245523.
25. K. Kobayashi, S. Nagase, *Organometallics* **16**, 2489 (1997).
26. N. Takagi, S. Nagase, *Eur. J. Inorg. Chem.* **2002**, 2775 (2002).
27. M. Ichinohe, M. Toyoshima, R. Kinjo, A. Sekiguchi, *J. Am. Chem. Soc.* **125**, 13328 (2003).
28. N. Wiberg, W. Niedermayer, G. Fischer, H. Nöth, M. Suter, *Eur. J. Inorg. Chem.* **2002**, 1066 (2002).

29. Supported by a Grant-in-Aid for Scientific Research (Nos. 134078204, 16205008, and 16550028) from the Ministry of Education, Science and Culture of Japan, and Center of Excellence program. We thank S. Nagase for helpful discussions and advice.

Supporting Online Material
www.sciencemag.org/cgi/content/full/305/5691/1755/DC1
Tables S1 to S5

30 June 2004; accepted 2 August 2004

A Linear, O-Coordinated η^1-CO_2 Bound to Uranium

Ingrid Castro-Rodriguez, Hidetaka Nakai, Lev N. Zakharov, Arnold L. Rheingold, Karsten Meyer*

The electron-rich, six-coordinate tris-aryloxide uranium(III) complex [((^{Ad}ArO)$_3$tacn)U^{III}] [where (^{Ad}ArOH)$_3$tacn = 1,4,7-tris(3-adamantyl-5-*tert*-butyl-2-hydroxybenzyl)1,4,7-triazacyclononane] reacts rapidly with CO_2 to yield [((^{Ad}ArO)$_3$tacn)U^{IV}(CO_2)], a complex in which the CO_2 ligand is linearly coordinated to the metal through its oxygen atom (η^1-O**CO). The latter complex has been crystallographically and spectroscopically characterized. The inequivalent O–C–O bond lengths [1.122 angstroms (Å) for the O–C bond adjacent to uranium and 1.277 Å for the other], considered together with magnetization data and electronic and vibrational spectra, support the following bonding model: U^{IV}=O=C$^{\bullet}$–O$^-$ ↔ U^{IV}–O≡C–O$^-$. In these charge-separated resonance structures, the uranium center is oxidized to uranium(IV) and the CO_2 ligand reduced by one electron.**

Carbon dioxide has been implicated as a main contributor to global warming because of its role in radiative forcing (*1*). However, CO_2 also represents an abundant renewable resource for the production of fine chemicals and clean fuels. Interest in metal-mediated multielectron reduction of CO_2 therefore remains high, but the molecule's inherent thermodynamic stability hinders the development of metal catalysts that achieve CO_2 activation and functionalization.

Particularly intriguing for synthetic chemists is the discovery of relatively simple coordination complexes that bind CO_2 and facilitate its reduction (*2*). Chemists have isolated and structurally characterized several synthetic metal complexes of CO_2, such as Aresta's archetypal [(Cy_3P)$_2$Ni(CO_2)] (Cy = cyclohexyl) (*3*, *4*) and Herskowitz's [(diars)$_2$M(CO_2)(Cl)] [diars = *o*-phenylenebis(dimethylarsine); M = Ir, Rh] (*5*), featuring the bidentate η^2-**CO**O and carbon-bound η^1-**C**O_2 binding modes, respectively. Activation of CO_2 via its adsorption on metal surfaces is of considerable interest for catalysis at the gas-surface interface (*6*, *7*). Most recently, Andrews and co-workers studied the interaction of CO_2 with a variety of transition (*8*) and actinide (*9*) metal atoms generated via laser ablation. Although C–O bond cleavage of a proposed intermediate η^2-**CO**O complex is predominant in these surface-adsorbed systems, there also is spectral evidence for η^1-**O**CO adsorption in low-temperature matrices (Scheme 1) (*8*). The most important CO_2 activation process occurs naturally during photosynthesis. It was proposed that during photosynthetic CO_2 fixation, an oxygen-coordinated CO_2 ligand (η^1-**O**CO) is enzymatically reduced by ribulose-1,5-bisphosphate carboxylase-oxygenase (RuBisCO) (*10*). Oxygen coordination appears to be an indispensable step for C-functionalization in this system. Recently, the relevance of the η^1-**O**CO coordination mode for biological systems was fueled by a crystallographic study on a deacetoxycephalosporin C synthase (DAOCS) mutant. The presence of electron density in proximity to the active site's iron center was found to be consistent with a monodentate O-bound CO_2 molecule (*11*). However, definitive structural characterization of inorganic coordination complexes with a linear oxygen-bound η^1-**O**CO coordination mode has remained elusive (*2*).

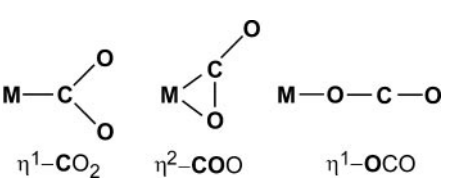

Scheme 1.

Department of Chemistry and Biochemistry, University of California, San Diego, 9500 Gilman Drive, MC 0358, La Jolla, CA 92093, USA.

*To whom correspondence should be addressed. E-mail: kmeyer@ucsd.edu